JPEE 2022
6as Jornadas Portuguesas de Engenharia de Estruturas
Encontro Nacional de Betão Estrutural 2022
12º Congresso Nacional de Sismologia e Engenharia Sísmica
Lisboa · LNEC · 9 a 11 de novembro de 2022

EXPERIMENTAL ANALYSIS OF THE OUT-OF-PLANE BEHAVIOUR OF A BRICK MASONRY WALL: PRELIMINARY RESULTS

Alberto Barontini

Researcher
University of Minho, ISISE, Department of Civil Engineering, Guimarães, Portugal
albe.barontini@mail.com

Jacopo Scacco

PhD student
Politecnico di Milano, Department ABC, Milan, Italy
balzac.js@gmail.com

Luis C. Silva

Assistant Professor
Politecnico di Milano, Department ABC, Milan, Italy
luiscarlos.martinsdasilva@polimi.it

Graça Vasconcelos

Assistant Professor
University of Minho, ISISE, Department of Civil Engineering, Guimarães, Portugal
graca@civil.uminho.pt

Paulo Lourenço

Full Professor
University of Minho, ISISE, Department of Civil Engineering, Guimarães, Portugal
pbl@civil.uminho.pt

ABSTRACT

Past earthquakes demonstrated that local out-of-plane collapses of brick masonry walls, particularly façades, are common even under moderate loads and a correct interpretation and assessment of their out-of-plane response is still a complex challenge. The present paper aims at contributing to the better understanding of clay brick masonry walls behaviour, through experimental analysis in laboratory environment. An extensive testing programme is carried out in the facility of the University of Minho, encompassing the characterisation of the mechanical properties of the materials through destructive and non-destructive techniques and a quasi-static test with airbag on a clay brick masonry specimen with U-shaped plan. Here, we present and discuss the preliminary results of such a thorough investigation.

Keywords: Brick masonry walls; Out-of-plane test; Material characterisation; Experimental analysis.

1. INTRODUCTION

Mechanical behaviour of masonry is strongly affected by its composite character, namely by the properties of the units (e.g. bricks or stones), the joints (e.g. dry or mortared) and unit-joints interfaces. The lower tensile and interface bond strength [1] make masonry structures particularly vulnerable to horizontal loading as, for instance, when subjected to seismic loading.

Nonetheless, Unreinforced Masonry (URM) buildings are among the most common traditional constructions, including in hazard-prone areas. Several advanced numerical strategies have been developed to simulate URMs structural behaviour and to predict their performance under different loading scenarios. There are still open issues despite the effectiveness and reliability of the design and assessment procedures [1][2]. Experimentation has a pivotal role, either by offering insight into the structural response under specific loading in a controlled environment and in providing data for the validation of numerical approaches. To this end, a thorough experimental campaign was designed and implemented in the laboratory facility of the University of Minho. The activities encompass the quasi-static out-of-plane destructive test of a U-shaped URM specimen, upon a detailed characterisation of the material properties by means of destructive and non-destructive evaluations. Here, the preliminary results of the material characterisation and testing are presented.

2. GEOMETRY AND CONSTRUCTION PROCESS

The U-shaped specimen (Figure 1) is composed of a front wall (2.9 m wide, 1.40 m high, 0.25 m thick) and two transverse walls (1.6 m wide, 1.40 m high, 0.25 m thick), with solid clay bricks (0.25×0.12×0.06 m^3). Pre-mixed cement-based mortar mixed with water, according to manufacturer recommendations, was used. Horizontal bed joints and the unaligned vertical joints were constructed with 10 mm of thickness.

After the completion of the wall specimen, a vertical static pressure load equal to 0.1 MPa was applied to the top of the side walls aiming the modelling of the typical weight of slabs and to prevent rocking of the lateral walls. Rocking and sliding of the concrete base is also avoided by anchoring two vertical shoring posts to the reinforced concrete reaction slab and four horizontal shoring posts to the reinforced concrete reaction wall.

(a) (b) (c)

Figure 1. U-shaped specimen: (a) axonometric view; (b) final construction stage; and (c) applied vertical load in transversal walls with the frame to support the airbag.

3. MATERIAL CHARACTERISATION

3.1 Mortar flexural and compressive strength

A total of nine mortar specimens were casted in a 4×4×16 cm^3 mould. These belong to three different working days. Compressive ($f_{b,c}$) and flexural ($f_{b,f}$) strength of the mortar were determined according to EN 1015-11 standard [3] (Figure 2). Table 1 reports the results found with average values of 1.5 and 3.6 N/mm^2 for $f_{b,c}$ and $f_{b,f}$, respectively.

Table 1. Results for the flexural and compression tests of mortar.

Day	$f_{b,f}$ [N/mm^2]	$f_{b,c}$ [N/mm^2]
01	1.6	3.7
02	1.4	3.6
03	1.6	3.5

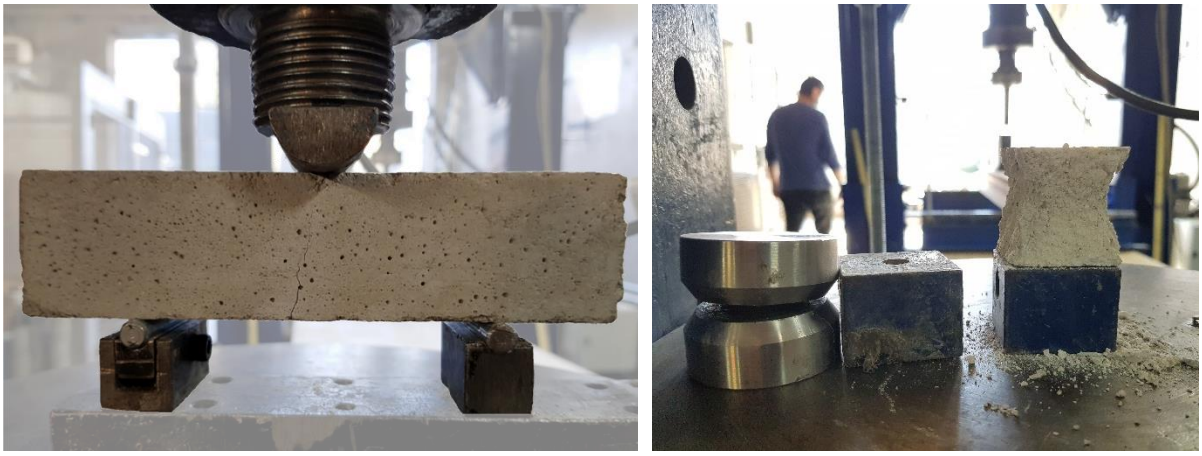

(a) **(b)**

Figure 2. Mortar specimens: (a) flexural test; (b) compression test.

3.2 Uniaxial compression test of masonry units

A total of three panels with eleven rows, each made of three bricks (approximately 0.75 m high × 0.40 m wide × 0.25 m thick), were built and tested according to the EN 1052-1 standard [4]. An uniform monotonic load was applied to the whole top face and the response was monitored with six Linear Variable Differential Transducers (LVDTs) (Figure 3). The compressive strength of each wallet is calculated as follows:

$$f_i = F_{i,max}/A_i \quad (1)$$

in which $F_{i,max}$ is the maximum compressive load reached during the test, and A_i is the loaded cross-section area of the specimen. The secant modulus at the point corresponding to one third of the maximum load was used to compute the Young's modulus:

$$E_i = F_{i,max}/(3\varepsilon_i A_i) \quad (2)$$

in which ε_i is the mean of the strains of all four measuring positions at one third of the maximum stress. Table 2 presents the results found and the values at two third and at the first crack are also reported for comparison purposes. The Poisson's coefficient that corresponds to one third of the maximum applied load is estimated as:

$$\nu = \frac{\varepsilon_{horizontal}}{\varepsilon_{vertical}} \tag{3}$$

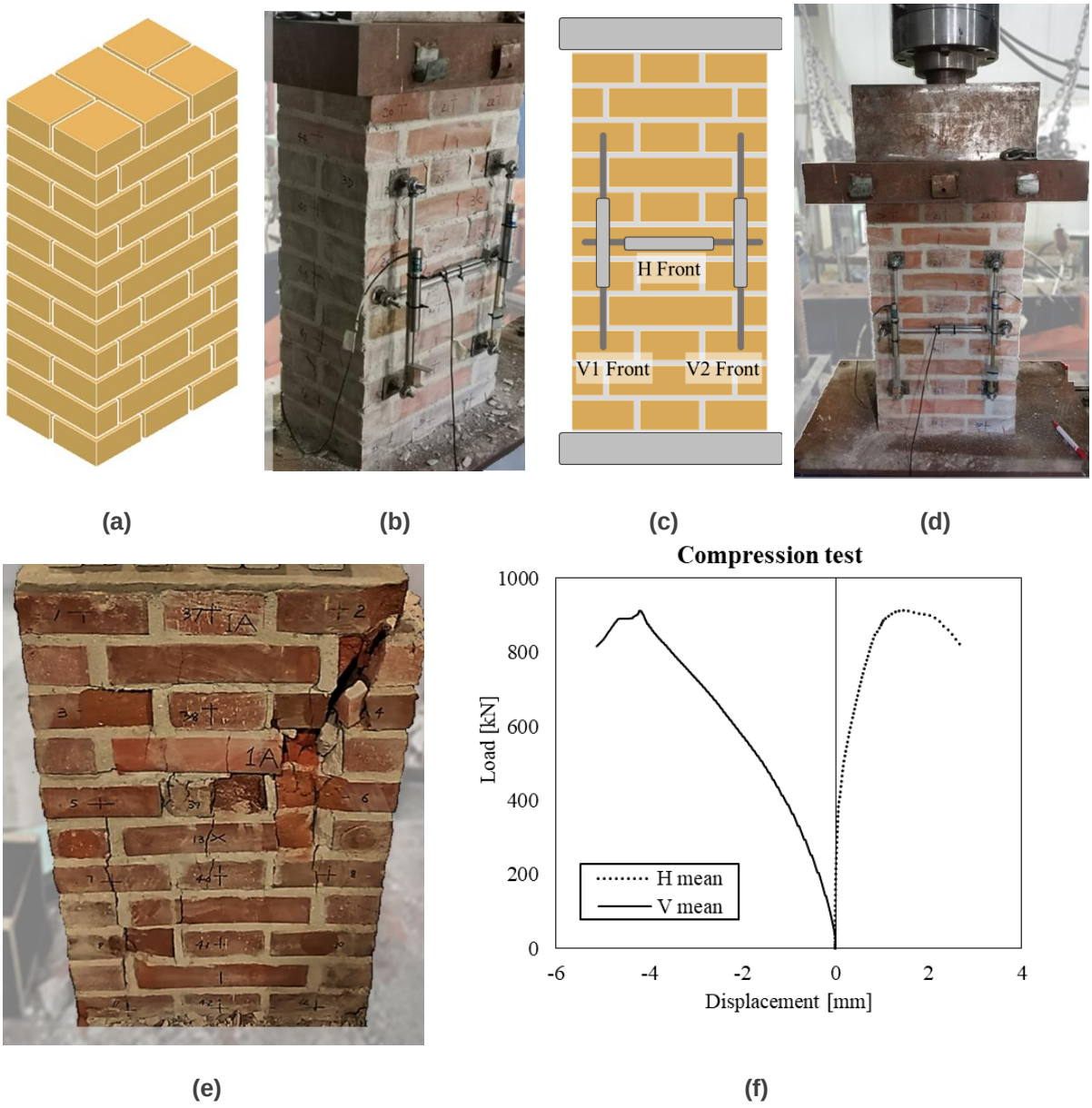

Figure 3. Wallets subjected to compression test: (a-d) specimen and test set-up; (e) W02 mode of failure; (f) W02 load-displacement curve.

The characteristic compressive strength of masonry is assumed equal to:

$$f_{k,c} = \min\left(\frac{f_{mean}}{1.2}, f_{i,min}\right) \tag{4}$$

which corresponds to 7.3 N/mm^2. The average Young's modulus and Poisson's ratio are 1800 N/mm^2 and 0.12, respectively.

Table 2. Results of the compression test.

Wallet	$F_{i,max}$ [kN]	$F_{i,crack}$ [kN]	f_i [N/mm^2]	$E_{i,1/3}$ [N/mm^2]	$E_{i,crack}$ [N/ mm^2]	$E_{i,2/3}$ [N/ mm^2]	v
01	813	450	8.1	1800	1450	1250	0.15
02	912.5	550	9.1	1800	1250	1150	0.11
03	903	350	9.0	1850	1300	1200	0.10

3.3 Uniaxial diagonal compression test of masonry units

Three panels were built and tested according to the ASTM E 519 standard [5] under monotonic load applied to the top corner. The response was monitored through four LVDTs (Figure 4) and the experimental shear strength calculated as:

$$\tau_{0,i} = \sigma_{0,i} = \frac{0.707 F_{i,max}}{A_{n,i}} \tag{5}$$

in which $F_{i,max}$ is the maximum compressive load reached during the test, and $A_{n,i}$ loaded cross-section area of the specimen. The angular deformation is estimated as:

$$\gamma_i = \frac{\Delta V_i + \Delta H_i}{g_i} \tag{6}$$

In which ΔV_i and ΔH_i are the diagonal shortening and extension, respectively; and g_i is the gage length. This value is used to estimate the shear modulus as:

$$G_i = \frac{\tau_{0,i}}{\gamma_i} \tag{7}$$

The latter data is collected and reported in Table 3.

Table 3. Results of the diagonal compression test.

Wallet	$F_{i,max}$ [kN]	$\tau_{0,i}$ [N/mm2]	G_i [N/mm^2]
W01	30.28	0.095	250
W02	47.61	0.150	400
W03	33.54	0.105	300

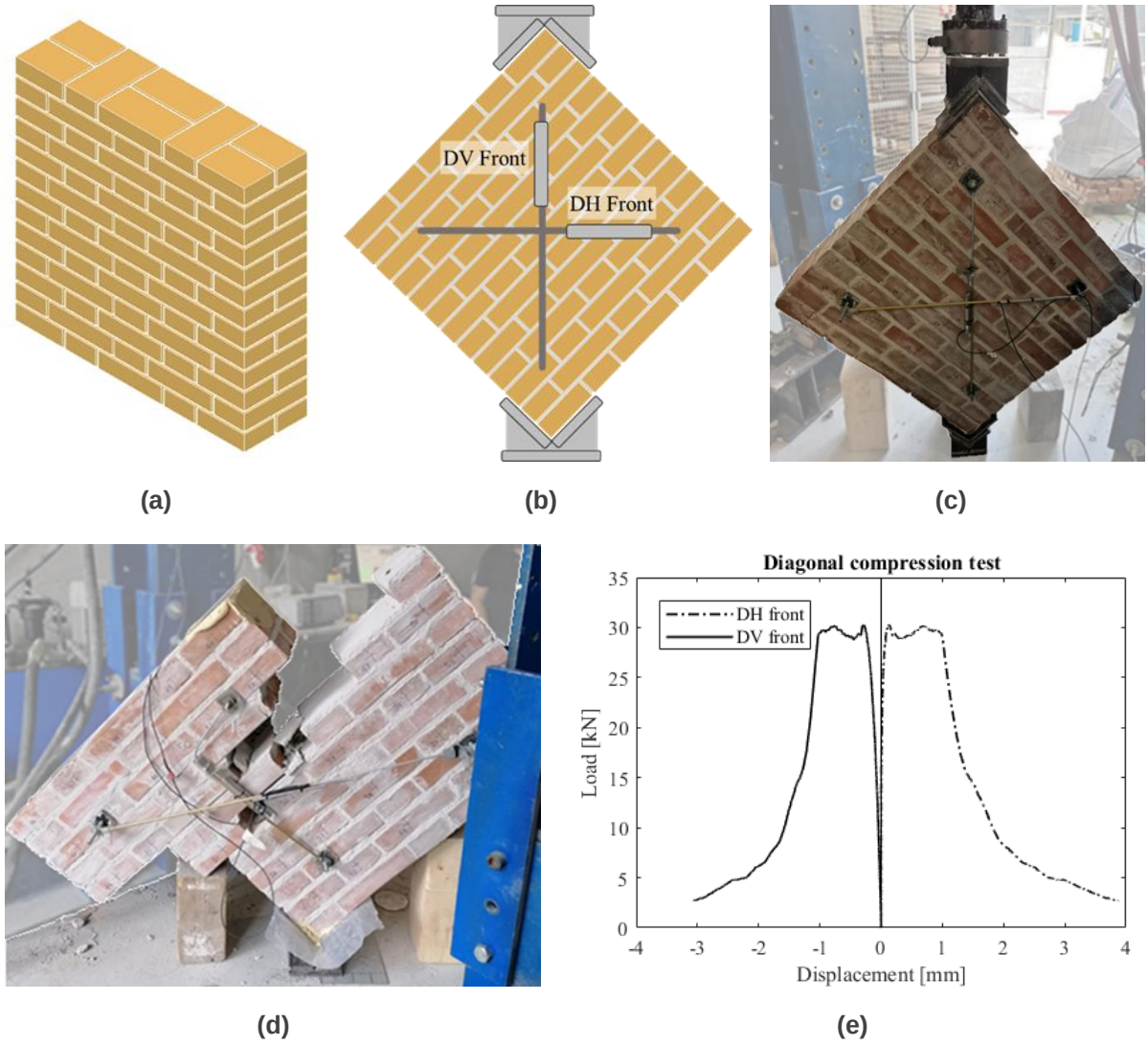

Figure 4. Diagonal compression test: (a-d) masonry specimen and test set-up; (e) failure mode for W02; and (f) load-displacement curve for W01.

3.4 Flexural test of masonry units

Four panels with 19 rows of 3 bricks each (approximately 1.30 m high × 0.50 m wide × 0.25 m thick) were built and tested to destruction according to EN 1052-2 standard [6], under monotonic load, recording the response through 6 LVDTs (Figure 5).

For each wallet, the flexural strength is:

$$f_{xi} = \frac{3F_{i,max}(l_1 - l_2)}{2bt_u^2} \tag{8}$$

where $F_{i,max}$ is the maximum load reached during the test, b is the width of the specimen, t_u is the width of the specimen, l_1 and l_1 are the distance between the outer and inner bearings, respectively.

The results are reported in Table 4. The characteristic flexural strength is calculated as:

$$f_{xk} = \frac{f_{mean}}{1.5} \quad (9)$$

corresponding to 0.04 N/mm^2.

Table 4. Results of the flexural test.

Wallet	$F_{i,max}$ [kN]	f_i [N/mm2]
01	1.65	0.06
02	1.62	0.06
03	1.71	0.06
04	1.21	0.04

(a) (b) (c)

Figure 5. Wallets subjected to flexural test: (a-b) specimen and test set-up; (c) W02 mode of failure.

4. OUT-OF-PLANE QUASI-STATIC CYCLIC TEST

The quasi-static out-of-plane load was applied through an airbag, which allows a uniform distribution of the horizontal thrust on the rear surface of the front wall. The airbag was placed between the specimen and a constraint structure, which is made of a timber board supported by a steel frame. The timber plank provides a smooth surface for the airbag. The frame can slide at the base on teflon sheets under the load induced by the airbag, which is pushed against the reinforced concrete reaction wall. Four load-cells placed between the frame and the reaction wall allowed the monitoring of the applied load.

The cyclic test was conducted under displacement control by inflating and deflating the airbag until reaching a pre-determined threshold. The control was evaluated for a point placed on the top of the front wall. The first cycle was repeated three times to ensure a first tuning and checking of the instruments and testing protocol. The other loading cycles were repeated two times only to assess the hysteretic behaviour under un-loading and re-loading phases. The

first step was equal to 0.5 mm; and the following steps were defined by increasing the previous displacement by 1.4 times, see Table 5.

Table 5. Test protocol: number of steps and repetitions, target maximum displacement of the control point and velocity of the loading-unloading cycle.

Step	Repetition	Displacement	Velocity
1	1	0.50	0.002
	2	0.50	0.002
	3	0.50	0.002
2	1	1.00	0.002
	2	1.00	0.002
3	1	1.40	0.002
	2	1.40	0.003
4	1	1.96	0.003
	2	1.96	0.003
5	1	2.74	0.003
	2	2.74	0.003
6	1	3.84	0.003
	2	3.84	0.003

Step	Repetition	Displacement	Velocity
7	1	5.38	0.005
	2	5.38	0.005
8	1	7.53	0.005
	2	7.53	0.005
9	1	10.54	0.01
	2	10.54	0.01
10	1	14.76	0.015
	2	14.76	0.015
11	1	20.66	0.015
	2	20.66	0.015
12	1	28.93	0.02
	2	28.93	0.02

The response of the specimen was monitored by twenty-three LVDTs; besides one that was placed in the control point. The location of the LVDTs was defined for several vertical alignments in the front wall aiming to: (i) identify the detachment of the front wall and the transverse walls, (ii) vertical detachment of the transverse walls regarding the base, and (iii) sliding or rocking at the base. It is noteworthy to recall that LVDTs were placed on the surface of units only.

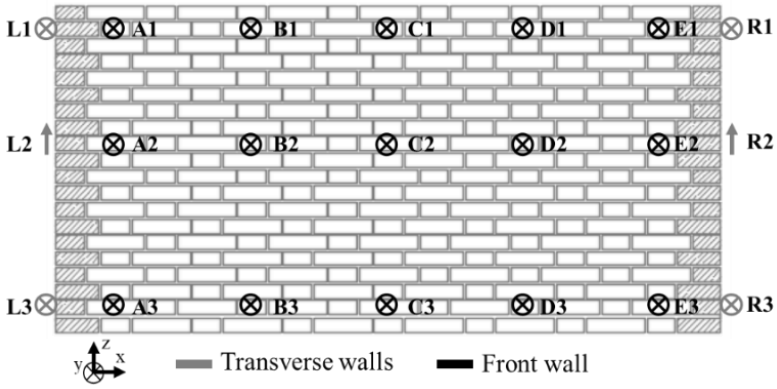

Figure 6. LVDTs locations.

The envelope curve of the force-displacement diagram is reported in Figure 7(a). Here, the displacement of the topmost measurement mid-point (point C1) was considered. An almost linear behaviour characterises the out-of-plane response until the peak load given by 54.39kN during the first repetition of the fourth step (1.96 mm). The onset of cracking occurred for such load level. After the peak, a progressively decreasing loading level emerges, with a faster softening in the first part of the curve followed by the existence of a plateau.

Crack pattern evolution in the front surface of the wall was also monitored. Owing to laboratory difficulties, the rear surface damage was only inspected after the completion of the test and it is presented in Figure 7(b). An almost vertical crack is clear from the top to the bottom of the front wall. It has a zig-zag shape as it follows the line of minimum trace governed by the mortar joints or unit-joints interfaces. A horizontal crack is also evident around one third of the wall height. The portion of the front wall above this crack presents evidence of sliding combined with an out-of-plane rotation. This displacement induced cracks in the internal face of the transverse walls around the connection with the front wall.

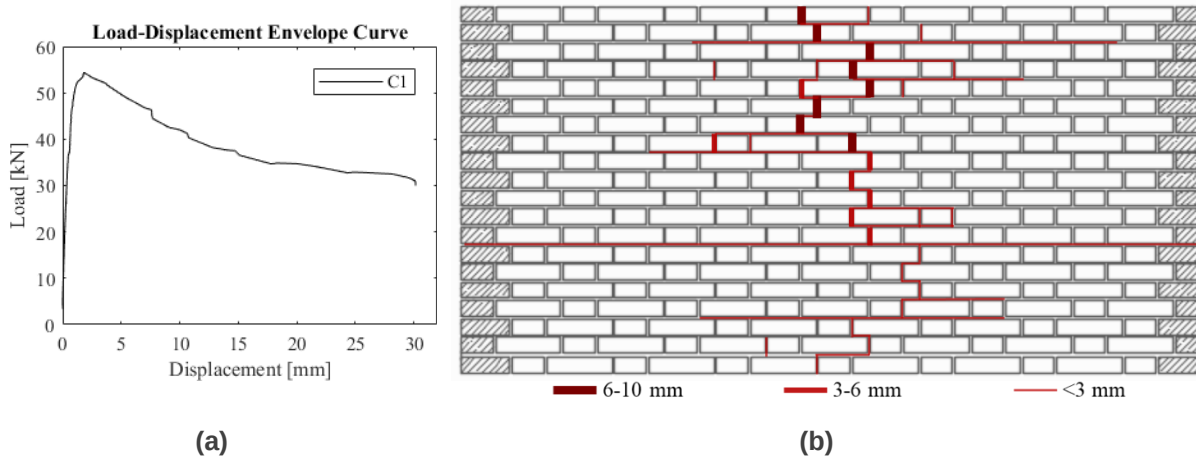

Figure 7. Test results: (a) envelope of the load-displacement curve at measurement point C1; (b) final damage pattern.

5. CONCLUSION

The study reported details on the out-of-plane quasi-static cyclic test, conducted in a laboratory environment, of a U-shaped unreinforced masonry wall featuring a Flemish-bond arrangement. The geometry details were addressed, together with the mechanical characterisation of the masonry components, according to well-established guidelines. The results from the quasi-static test with airbag on the U-shaped wall were presented and discussed for both the load-displacement envelope and failure pattern.

ACKNOWLEDGEMENTS

This work was financed by FCT/MCTES through national funds (PIDDAC), within the scope of the project “RESIST-2020 – Seismic Rehabilitation of Old Masonry-Concrete Buildings” (PTDC/ECI-EGC/30567/2017). This work was partly financed by FCT/MCTES through national funds (PIDDAC) under the R&D Unit Institute for Sustainability and Innovation in Structural Engineering (ISISE), under reference UIDB/04029/2020.

REFERENCES

[1] P. Roca, M. Cervera, G. Gariup, and L. Pela – "Structural Analysis of Masonry Historical Constructions. Classical and Advanced Approaches", *Arch Computat Methods Eng*, vol. 17, no. 3, Sep. 2010, p. 299-325, doi: 10.1007/s11831-010-9046-1.

[2] P. B. Lourenço and R. Marques – "Design of masonry structures (General rules): Highlights of the new European masonry code", in *Brick and Block Masonry-From Historical to Sustainable Masonry*, CRC Press, 2020, p. 3-17.

[3] EN 1015-11: "Methods of test for mortar for masonry Determination of flexural and compressive strength of hardened mortar". 2019.

[4] EN 1052-1: "Methods of Test for Masonry - Part 1: Determination of Compressive Strength". 1999.

[5] ASTM E519/E519M-21: "Standard Test Method for Diagonal Tension (Shear) in Masonry Assemblages". 2021.

[6] EN 1052-2: "Methods of test for masonry Determination of flexural strength". 2017.